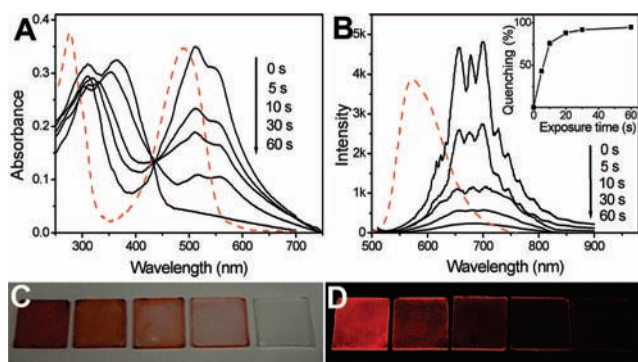




between the experimental tilting angles along the zone axis and those recalculated (in parentheses) based on the unit cell parameters corresponding to the diffraction patterns in Figure 2B. The nanowire axis was found to be along the [100] direction, which is the same direction pointing from the transmitted spot to the (100) spot in the diffraction patterns (Figure 2B). In addition, the XRD pattern of DAAQ nanowires also showed a preferred orientation of the (100) plane (Figure S2). The XRD pattern of the nanowires matched the powder pattern except for the relative peak intensities, suggesting that DAAQ did not undergo phase transition or chemical reaction during the vapor transport.

Since the organic nanowires were made without catalysts or liquid droplets as is needed in the vapor–liquid–solid synthesis for many inorganic nanowires, the growth should be controlled by a vapor–solid condensation process. To observe the early stage of nanowire growth, the deposition was stopped within seconds. SEM observation of the substrates revealed that DAAQ first deposited as well-separated nanoparticles of  $\sim 100$  nm in diameter (Figure S3) with a density comparable to that of the final nanowire arrays. This indicates that the nanowires were grown on these seed nanoparticles. Crystallographic studies on such nanoparticles grown on  $\text{SiO}_x$  coated copper grids were carried out in TEM by electron diffraction. When viewed from the bottom, the cross section of the nanoparticles was perpendicular to the electron beam. The electron diffraction pattern could be indexed along the [100] zone axis (Figure 2C). When tilted off to nearly  $90^\circ$ , the electron diffraction pattern (Figure 2D) again shows the (100) spot, which confirms that the growth direction was along the [100] direction. Since vertical nanowires were obtained on many different substrates, it implies that the vapor may have condensed to form similarly oriented seeds on those surfaces as well.

The intramolecular charge transfer between the neighboring amine and carbonyl groups is responsible for the color and fluorescence of DAAQ. In an ethanol solution, the molecules exhibit two resolved absorption bands at 275 and 490 nm, respectively (Figure 3A, red line).



**Figure 3.** Time dependent absorption (A) and PL (B) spectra of the DAAQ nanowire arrays on exposure to the HCl vapor (*ca.* 5 ppm in air). The red dashed lines are the spectra of diluted DAAQ solution in ethanol. The inset in (B) shows the PL intensity at 675 nm over time. (C and D) Photographs showing samples exposed to HCl for 0, 5, 10, 30, and 60 s, respectively. (C) was taken under bright field illumination, and (D) was taken under dark field excitation by blue light (460–490 nm). The blue background color in (D) was removed to better match the observation by eye. The color changes observed in (C, D) were consistent with the changes in the spectra in (A, B).

The UV band is attributed to the  $\pi \rightarrow \pi^*$  type  $2^1B_u \leftarrow X^1A_g$  transition, while the visible band is assigned as the  $1^1B_u \leftarrow X^1A_g$  transition, which is also  $\pi \rightarrow \pi^*$  type and has a predominant intramolecular charge transfer character.<sup>13</sup> Both bands exhibited a red shift in the nanowires due to the molecular aggregation. Since the charge transfer can be interrupted if the N atoms are protonated, we carried out acid sensing experiments based on the changes in color and fluorescence on

exposure to  $\sim 5$  ppm of HCl vapor in air. Figure 3A shows the absorption spectra of the nanowire arrays after being exposed to HCl for different lengths of time. The visible band rapidly decreased accompanied by apparent bleaching of the red color of the sample (Figure 3C). The photoluminescence (PL) spectrum of free DAAQ molecules in ethanol shows an approximately symmetric peak centered at 575 nm, whereas the nanowire arrays displays a super broadband emission from 500 to 900 nm (Figure 3B). On exposure to HCl, the PL intensity rapidly decreased, reaching over 90% quenching after only 30 s. Fluorescence quenching can be seen by eye when the samples were illuminated with blue light (460–490 nm) (Figure 3D). In a control experiment, DAAQ powders composed of micron sized particles did not show an apparent response even after 30 min of exposure (Figure S4).

Both the absorption and PL can be recovered in air to  $\sim 95\%$  of their original intensity in  $\sim 2$  h. However, they can be rapidly reset by basic vapors (e.g.,  $\text{NH}_3$ ) within 2 s. This also provides a mechanism for detecting basic vapors. The basic vapor deprotonated the amine groups and helped to restore the intramolecular charge transfer, leading to the recovery of color and fluorescence (Figure S5). The nanowires were exposed to cycles of acid and base vapors. A good consistency in the bleaching and quenching efficiencies (Figure S6) was observed.

In summary, vertical organic nanowire arrays of DAAQ dye molecules were prepared by a facile physical vapor transport method. The crystal structure and growth direction of the nanowires were determined by TEM and electron diffraction. These fluorescent nanowires were sensitive to acidic and basic vapors. The ease of oriented vertical growth should make it possible to directly integrate these nanowires into photonic sensing devices.<sup>14</sup>

**Acknowledgment.** The work was supported by a seed grant from the NU-NSEC (NSF EEC-0647560) and an ACS-PRF grant (48678-G10). TEM work was performed in the EPIC facility of the NUANCE center at Northwestern.

**Supporting Information Available:** Materials and methods; More SEM images of the nanowires; XRD patterns of the nanowires and bulk DAAQ; SEM images of the nucleation stage; Sensing performance of DAAQ powder; Pictures showing color and fluorescence changes of the nanowires on exposure to HCl and  $\text{NH}_3$ ; PL quenching–recovery circles. This material is available free of charge via the Internet at <http://pubs.acs.org>.

## References

- (1) Law, M.; Greene, L. E.; Johnson, J. C.; Saykally, R.; Yang, P. *Nat. Mater.* **2005**, *4*, 455.
- (2) Chan, C. K.; Peng, H.; Liu, G.; McIlwrath, K.; Zhang, X. F.; Huggins, R. A.; Cui, Y. *Nat. Nanotechnol.* **2008**, *3*, 31.
- (3) Chen, J. J.; Wang, K.; Hartman, L.; Zhou, W. *J. Phys. Chem. C* **2008**, *112*, 16017.
- (4) Lee, C. -Y.; Lu, M. -P.; Liao, K. -F.; Wu, W. -W.; Chen, L. -J. *Appl. Phys. Lett.* **2008**, *93*, 113109.
- (5) Lai, E.; Kim, W.; Yang, P. *Nano Res.* **2008**, *1*, 123.
- (6) Goldberger, J.; Hochbaum, A.; Fan, R.; Yang, P. *Nano Lett.* **2006**, *6*, 973.
- (7) Huang, M.; Mao, S.; Feick, H.; Yan, H.; Wu, Y.; Kind, H.; Weber, E.; Russo, R.; Yang, P. *Science* **2001**, *292*, 1897.
- (8) Wang, Z. L.; Song, J. *Science* **2006**, *312*, 342.
- (9) (a) Zang, L.; Che, Y.; Moore, J. S. *Acc. Chem. Res.* **2008**, *41*, 1596. (b) Briseno, A. L.; Mannsfeld, S. C. B.; Lu, X.; Xiong, Y.; Jenekhe, S. A.; Bao, Z.; Xia, Y. *Nano Lett.* **2007**, *7*, 668. (c) Zhao, Y. S.; Fu, H.; Peng, A.; Ma, Y.; Xiao, D.; Yao, J. *Adv. Mater.* **2008**, *20*, 2859. (d) Al-Kaysi, R. O.; Müller, A. M.; Bardeen, C. J. *J. Am. Chem. Soc.* **2006**, *128*, 15938.
- (10) Patai, S. *The Chemistry of the Quinonoid Compounds*; Wiley: New York, 1974.
- (11) (a) Liu, H.; Li, Y.; Xiao, S.; Gan, H.; Jiu, T.; Li, H.; Jiang, L.; Zhu, D.; Yu, D.; Xiang, B.; Chen, Y. *J. Am. Chem. Soc.* **2003**, *125*, 10794. (b) Debe, M. K.; Drube, A. R. *J. Vac. Sci. Technol., B* **1995**, *13*, 1236.
- (12) Wu, J.; Spence, J. C. *J. Appl. Crystallogr.* **2004**, *37*, 78.
- (13) Khan, M. S.; Khan, Z. H. *Spectrochim. Acta A* **2003**, *59*, 1409.
- (14) He, R.; Yang, P. *Nat. Nanotechnol.* **2006**, *1*, 42.

JA809360V